



HAL
open science

Data-Driven Stabilization of Input-Saturated Systems

Valentina Breschi, Luca Zaccarian, Simone Formentin

► **To cite this version:**

Valentina Breschi, Luca Zaccarian, Simone Formentin. Data-Driven Stabilization of Input-Saturated Systems. IEEE Control Systems Letters, 2023, 7, pp.1640-1645. 10.1109/LCSYS.2023.3266254 . hal-04117896

HAL Id: hal-04117896

<https://laas.hal.science/hal-04117896>

Submitted on 5 Jun 2023

HAL is a multi-disciplinary open access archive for the deposit and dissemination of scientific research documents, whether they are published or not. The documents may come from teaching and research institutions in France or abroad, or from public or private research centers.

L'archive ouverte pluridisciplinaire **HAL**, est destinée au dépôt et à la diffusion de documents scientifiques de niveau recherche, publiés ou non, émanant des établissements d'enseignement et de recherche français ou étrangers, des laboratoires publics ou privés.

Data-driven stabilization of input-saturated systems

Valentina Breschi, *Member, IEEE*, Luca Zaccarian, *Fellow, IEEE*, and Simone Formentin, *Member, IEEE*

Abstract—We provide a data-driven stabilization approach for input-saturated systems with formal Lyapunov guarantees. Through a generalized sector condition, we propose a convex design algorithm based on linear matrix inequalities for obtaining a regionally stabilizing data-driven static state-feedback gain. Regional, rather than global, properties allow us to address non-exponentially stable plants, thereby making our design broad in terms of applicability. Moreover, we discuss consistency issues and introduce practical tools to deal with measurement noise. Numerical simulations show the effectiveness of our approach and its sensitivity to the features of the dataset.

Index Terms—data-driven control, input saturation

I. INTRODUCTION

Data-driven (DD) control is recently enjoying great success as an alternative to traditional model-based design. In particular, existing DD control techniques range from model-reference approaches, *e.g.*, [5], [10], to the recently proposed optimal (*e.g.*, [8], [9]) and predictive techniques [2], [6]. Nonetheless, few solutions have been devised to handle systems with input saturation apart from predictive strategies. Moreover, these alternatives to predictive control have mainly been tailored to the model-reference framework. Indeed, a VRFT-like strategy is proposed in [3], where saturation is accounted for by augmenting the cost of the optimization problem solved to design a fixed-structure (dynamic) controller. A similar principle is exploited in [4], where a neural network controller is used to cope with input saturation. However, neither of these solutions provides stability guarantees. On the other hand, the MPC-based DD solution in [1] provides robust stability guarantees, but does not account for input saturation that would otherwise prevent global results to be achieved with general (possibly exponentially unstable) plants. In the model-based context, several tools are instead available, mostly stemming from generalized sector conditions leading to regional stability guarantees (with guaranteed estimates of the basin of attraction) with easily implementable feedbacks [14], [17] and less cumbersome online computations, as compared to MPC.

This project was partially supported by the Italian Ministry of University and Research under the PRIN'17 project "Data-driven learning of constrained control systems", contract no. 2017J89ARP.

V. Breschi is with Dept. of Electrical Engineering, Eindhoven University of Technology, Eindhoven, Netherlands. L. Zaccarian is with LAAS-CNRS, University of Toulouse, France, and also with Dip. di Ing. Industriale, Università di Trento, Italy. S. Formentin is with Dip. di Elettronica, Informazione e Bioingegneria, Polit. di Milano, Italy (e-mail: simone.formentin@polimi.it).

In this note, we exploit generalized sector conditions to propose a novel DD solution for the design of regionally stabilizing controllers for input-saturated systems. To this end, we introduce a DD formulation of the model-based solutions in [14], starting from a behavioral description of linear systems [16] and its closed-loop counterpart [7]. Assuming the state to be fully accessible, the DD solution solely requires the explicit identification of the matrix B linking the state evolution to the input. By working at the boundary between system identification and control design, we thus need to identify how the nonlinearity (*i.e.*, the saturation) affects the system.

To handle noisy data, we propose to use an instrumental variable scheme [12]. A similar approach has been used for the design of DD predictive controllers [15]. With this well-known tool in system identification, we are able to recover an (asymptotically) unbiased description of the closed-loop system (in line with the one in [15]), which is ultimately exploited to design the regionally stabilizing feedback law.

The paper is organized as follows. The problem statement is given in Section II. A first solution is given in Section III, in a deterministic setting. The issues stemming from using a deterministic solution within a noisy setting are then discussed in Section IV, where a design strategy with noisy data is then proposed. Section V shows some numerical results, highlighting the potential of the proposed framework.

Notation. For a full-row-rank matrix Y , Y^\dagger denotes its right pseudo-inverse. For matrix $A \in \mathbb{R}^{n_x \times n_x}$, $\text{He}(A) = A + A^\top$. $x^+ = Ax$ is a shorthand for $x(t+1) = Ax(t)$. Given another sequence $t \mapsto w(t) \in \mathbb{R}^{n_w}$, for any $0 \leq t_0 < t_1 \leq T$ and $1 \leq \tau < t_1$, we define the associated Hankel matrix as

$$W_{t_0, \tau, t_1} = \begin{bmatrix} w(t_0) & w(t_0+1) & \cdots & w(t_1-\tau) \\ w(t_0+1) & w(t_0+2) & \cdots & w(t_1-\tau+1) \\ \vdots & \vdots & \ddots & \vdots \\ w(t_0+\tau-1) & w(t_0+\tau) & \cdots & w(t_1-1) \end{bmatrix} \quad (1)$$

while we denote the single row Hankel matrix as follows:

$$W_{t_0, t_1} = W_{t_0, 1, t_1} = [w(t_0) \quad w(t_0+1) \quad \cdots \quad w(t_1)]. \quad (2)$$

Definition 1 (Persistence of excitation): A sequence $w(t) \in \mathbb{R}^{n_w}$ is persistently exciting of order τ if the Hankel matrix W_{t_0, τ, t_1} in (1) is full row rank, namely $\text{rank}(W_{t_0, \tau, t_1}) = \tau \cdot n_w$.

II. PROBLEM FORMULATION

Consider a discrete-time, *linear time-invariant* (LTI) and *controllable* plant \mathcal{P} , in cascade with an input saturation. Let this cascade be described by the difference equation

$$x^+ = Ax + Bv = Ax + B \text{sat}(u), \quad (3a)$$

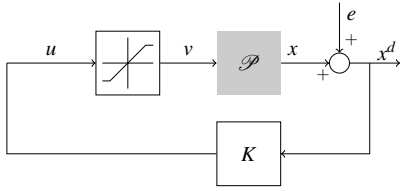


Fig. 1. Scheme of the (noisy) closed-loop system, where known/tunable blocks are depicted in white and the unknown plant is depicted in grey.

where $x \in \mathbb{R}^{n_x}$ is the state, $u \in \mathbb{R}^{n_u}$ is the input to the saturation, and $A \in \mathbb{R}^{n_x \times n_x}$ and $B \in \mathbb{R}^{n_x \times n_u}$ are *unknown* matrices of suitable dimensions. The input nonlinearity $\text{sat} : \mathbb{R}^{n_u} \rightarrow \mathbb{R}^{n_u}$ is a known decentralized saturation, whose components are defined as

$$v_i = \text{sat}_i(u_i) = \max\{-\bar{u}_{i,n}, \min\{\bar{u}_{i,p}, u_i\}\}, \quad i = 1, \dots, n_u, \quad (3b)$$

whose *known* lower and upper saturation bounds, gathered in vectors $\bar{u}_n, \bar{u}_p \in \mathbb{R}^m$, respectively, satisfy the component-wise inequalities $\bar{u}_n \geq \bar{u}$ and $\bar{u}_p \geq \bar{u}$ for some vector $\bar{u} = [\bar{u}_1 \ \dots \ \bar{u}_{n_u}]^\top \in \mathbb{R}^{n_u}$ having positive elements. Assume that we have access to *noisy* measurements of the state, *i.e.*,

$$x^d = x + e, \quad (4)$$

where $x^d \in \mathbb{R}^{n_x}$ denotes the measured state, and $e \in \mathbb{R}^{n_x}$ is a *zero mean*, white noise corrupting the *true* state x , here assumed to be uncorrelated to the inputs.

Even though A and B in (3a) are unknown, assume that we can carry out experiments on \mathcal{P} for data collection purposes. Specifically, suppose that we can feed the plant with a finite input sequence $\mathcal{V}_T = \{v^d(t)\}_{t=0}^{T-1}$, saturated in accordance with (3b), that is *persistently exciting* of order $n_x + 1$ according to Definition 1, and that we can collect the corresponding (noisy) states $\mathcal{X}_T = \{x^d(t)\}_{t=0}^T$. Given the dataset $\mathcal{D}_T = \{\mathcal{V}_T, \mathcal{X}_T\}$, **our goal is propose a data-based solution alternative to existing (and viable) system identification+model-based approaches**, to design a static state-feedback law, namely

$$u = Kx, \quad K \in \mathbb{R}^{n_u \times n_x}, \quad (5)$$

such that the origin of the closed loop in Fig. 1 is exponentially stable, while obtaining an (inner) estimate of the basin of attraction of the closed-loop system.

Remark 1 (On experiment design): For the rank condition in Definition 1 to be satisfied by the saturated input sequence \mathcal{V}_T , the user-defined inputs $\mathcal{U}_T = \{u^d(t)\}_{t=0}^T$ from which \mathcal{V}_T is originated ($v^d(t) = \text{sat}(u^d(t))$ for all t) should be chosen to avoid recurrent saturations as much as possible so that the input values are sufficiently rich to provide excitation.

III. DETERMINISTIC DATA-DRIVEN DESIGN OF REGIONALLY STABILIZING STATE-FEEDBACK LAWS

We initially focus on a *noiseless setting*, *i.e.*, $e = 0$ in (4), to show how a regionally stabilizing static state feedback law can be designed from data, using the generalized sector condition in [14]. As in the linear case [7], initially considering this simplified framework allows us to obtain DD conditions that are equivalent to their model-based counterparts.

At the core of our formulation lays the following foundational result, that stems directly from our setup and the fundamental lemma in [16].

Lemma 1: Given the input sequence \mathcal{U}_T in the available dataset \mathcal{D}_T , assume that $\mathcal{V}_T = \{v^d(t)\}_{t=0}^{T-1}$, is *persistently exciting* of order $n_x + 1$ and that the dataset length T satisfies

$$T \geq (n_u + 1)n_x + n_u \quad (6)$$

(namely, it is *sufficiently long*). Then, the following rank condition holds:

$$\text{rank} \left(\begin{bmatrix} V_{0,T-1}^d \\ X_{0,T-1}^d \end{bmatrix} \right) = n_u + n_x. \quad (7)$$

A. Characterizing the closed-loop dynamics from data

In a noise-free setting, the model-based representation (3a) is equivalent to the following DD characterization:

$$x^+ = \begin{bmatrix} B & A \end{bmatrix} \begin{bmatrix} \text{sat}(u) \\ x \end{bmatrix} = X_{1,T}^d \begin{bmatrix} V_{0,T-1}^d \\ X_{0,T-1}^d \end{bmatrix}^\dagger \begin{bmatrix} \text{sat}(u) \\ x \end{bmatrix}, \quad (8)$$

with $X_{1,T}^d = [x^d(1) \ \dots \ x^d(T)]$, as stated next.

Lemma 2 (DD open-loop with saturation): Given the *unknown* system in (3a) and a set of sufficiently long (in the sense of (6)) *noiseless* data $\mathcal{D}_T = \{\mathcal{V}_T, \mathcal{X}_T\}$, with \mathcal{V}_T being persistently exciting of order $n_x + 1$, the dynamics in (3a) can be equivalently characterized from data as in (8).

Proof: As in [7, Section III.A], the proof straightforwardly follows from the definition

$$\begin{bmatrix} B & A \\ B & A \end{bmatrix} = \underset{[B \ A]}{\text{argmin}} \left\| X_{1,T}^d - \begin{bmatrix} B & A \\ B & A \end{bmatrix} \begin{bmatrix} V_{0,T-1}^d \\ X_{0,T-1}^d \end{bmatrix} \right\|_F = X_{1,T}^d \begin{bmatrix} V_{0,T-1}^d \\ X_{0,T-1}^d \end{bmatrix}^\dagger, \quad (9)$$

thanks to the rank property in (7). ■

Introduce the dead-zone nonlinearity $\text{dz}(u) = u - \text{sat}(u)$ induced by sat , with u defined in (5). Starting from the identification-like result in Lemma 2, we provide the following data-based representation of the closed-loop (3), (5):

$$x^+ = X_{1,T}^d G^x x - X_{1,T}^d \begin{bmatrix} V_{0,T-1}^d \\ X_{0,T-1}^d \end{bmatrix}^\dagger \begin{bmatrix} \text{dz}(Kx) \\ 0 \end{bmatrix}, \quad (10)$$

with $G^x \in \mathbb{R}^{(T-1) \times n_x}$ satisfying

$$X_{0,T-1}^d G^x = I. \quad (11)$$

This result can be formalized as follows.

Lemma 3 (DD closed-loop with saturation): Given the *unknown* system in (3), and a sufficiently long (in the sense of (6)) set of *noiseless* data $\mathcal{D}_T = \{\mathcal{V}_T, \mathcal{X}_T\}$, with \mathcal{V}_T being persistently exciting of order $n_x + 1$, the closed loop (3), (5) is equivalent to (10), (11).

Proof: Replacing $\text{sat}(u) = \text{sat}(Kx) = Kx - \text{dz}(Kx)$ and applying Lemma 2, the closed loop (8), (5) can be written as

$$\begin{aligned} x^+ &= \begin{bmatrix} B & A \end{bmatrix} \begin{bmatrix} Kx \\ x \end{bmatrix} - X_{1,T}^d \begin{bmatrix} V_{0,T-1}^d \\ X_{0,T-1}^d \end{bmatrix}^\dagger \begin{bmatrix} \text{dz}(Kx) \\ 0 \end{bmatrix} \\ &= \begin{bmatrix} B & A \end{bmatrix} \begin{bmatrix} K \\ I \end{bmatrix} x - X_{1,T}^d \begin{bmatrix} V_{0,T-1}^d \\ X_{0,T-1}^d \end{bmatrix}^\dagger \begin{bmatrix} \text{dz}(Kx) \\ 0 \end{bmatrix}. \end{aligned} \quad (12)$$

Proceeding as in [7], the rank condition in (7) enables introducing a new variable $G^x \in \mathbb{R}^{(T-1) \times n_x}$, satisfying

$$\begin{bmatrix} K \\ I \end{bmatrix} = \begin{bmatrix} V_{0,T-1}^d \\ X_{0,T-1}^d \end{bmatrix} G^x, \quad (13)$$

whose existence is guaranteed by the Rouché-Capelli theorem. Substituting (13) into (12), the closed-loop representation (10) and the consistency characterization (11) follow. ■

Note that, according to (13), the static state-feedback gain K in (5) can be uniquely computed from G^x as

$$K = V_{0,T-1}^d G^x. \quad (14)$$

The data-based closed-loop representation in (10) can be then equivalently recast compactly as follows:

$$x^+ = A_{\text{cl}}^d(G^x)x - B_{\text{cl}}^d \text{dz}(Kx), \quad (15a)$$

where G^x should satisfy the consistency condition (11) and

$$A_{\text{cl}}^d(G^x) = X_{1,T}^d G^x, \quad B_{\text{cl}}^d = X_{1,T}^d \begin{bmatrix} V_{0,T-1}^d \\ X_{0,T-1}^d \end{bmatrix}^\dagger \begin{bmatrix} I \\ 0 \end{bmatrix}. \quad (15b)$$

It is thus clearer from (15) that the state transition matrix $A_{\text{cl}}^d(G^x)$ of the closed-loop depends on the data and on the variable G^x , which plays the role of *design parameter*, while we need to exploit the estimate B_{cl}^d of the matrix B in (8) to characterize the impact of the nonlinearity on the closed loop.

B. Regionally stabilizing static state feedback

To derive a design algorithm for a regionally stabilizing K in (5), let us recall the *regional sector condition* [14] for the dead-zone nonlinearity appearing in (15a), namely

$$\text{dz}(Hx) = 0 \implies \text{dz}(u)^\top W(u - \text{dz}(u) + Hx) \geq 0, \quad (16)$$

which holds for any $H \in \mathbb{R}^{n_u \times n_x}$, any $u \in \mathbb{R}^{n_u}$, and any positive definite *diagonal* matrix $W \in \mathbb{R}^{n_u \times n_u}$. Exploiting the quadratic Lyapunov function candidate

$$V(x) = x^\top Px, \quad (17)$$

with $P \in \mathbb{R}^{n_x \times n_x}$ being symmetric and positive definite, we cast the DD design K in (5) by solving the following *linear matrix inequality* (LMI) in the decision variables $Q = Q^\top = P^{-1}$, $M = W^{-1}$ diagonal, $F = G^x Q \in \mathbb{R}^{(T-1) \times n_x}$ and $N \in \mathbb{R}^{n_u \times n_x}$:

$$\begin{bmatrix} Q & N_j^\top \\ N_j & \tilde{u}_j^2 \end{bmatrix} \geq 0, \quad j = 1, \dots, n_u, \quad (18a)$$

$$\text{He} \begin{bmatrix} -\frac{Q}{2} & 0 & 0 \\ V_{0,T-1}^d F + N & -M & 0 \\ X_{1,T}^d F & -B_{\text{cl}}^d M & -\frac{Q}{2} \end{bmatrix} < 0, \quad (18b)$$

(where N_j denotes the j -th row of matrix N and B_{cl}^d only depends on data, as defined in (15b)) together with the consistency condition

$$X_{0,T-1}^d F = Q. \quad (18c)$$

The n_u LMIs in (18a) have dimension $n_x + 1$ each, while LMI (18b) has dimension $2n_x + n_u$, thus depending on the order of the system and the dimension of the input. Overall, also the size of the decision variables depends on the system's

features (and not on the length of the dataset), due to Q , W and N amounting to $\frac{n_x(n_x+1)}{2} + n_u + n_u n_x$ variables. Only F of size $(T-1)n_x$ depends on the length of the dataset, eventually making the proposed approach computationally more demanding than traditional design when a large dataset is available. This is the price to pay to avoid a full identification step.

We state below our noise-free DD design result.

Theorem 1 (Regionally stabilizing DD design): Given (3) and a noise free set of data \mathcal{D}_T satisfying the conditions in (6) and (7), if there exist matrices $Q = Q^\top$, M diagonal, $F \in \mathbb{R}^{(T-1) \times n_x}$ and $N \in \mathbb{R}^{n_u \times n_x}$ satisfying (18), then the following gain selection in (5)

$$K = V_{0,T-1}^d F Q^{-1}, \quad (19)$$

guarantees exponential stability of the origin for the closed loop (3), (5) with basin of attraction containing the set

$$\mathcal{E}(Q, 1) = \{x \in \mathbb{R}^{n_x} : x^\top Q^{-1} x \leq 1\}, \quad (20)$$

of Lyapunov function V in (17), with selection $P = Q^{-1}$.

Proof: Using the Lyapunov function candidate (17) with $P = P^\top = Q^{-1}$, which is positive definite due to the (1,1) entry in (18b), we may study exponential stability of the origin by studying the sign of the increment

$$\Delta V(x) = (x^+)^\top P x^+ - x^\top P x. \quad (21)$$

Starting from the solution Q, F, M, N of (18) assumed in the theorem statement, select $G^x = F Q^{-1}$ so that, from (18c) the consistency condition (11) is satisfied. Due to the consistency condition and since (19) matches the assumed selection (14), apply Lemma 3 to characterize the increment in (21) by the following DD inequality, issued from (15),

$$\begin{aligned} \Delta V(x) &= \\ &= \left(A_{\text{cl}}^d(G^x)x - B_{\text{cl}}^d \text{dz}(u) \right)^\top P \left(A_{\text{cl}}^d(G^x)x - B_{\text{cl}}^d \text{dz}(u) \right) - x^\top P x \\ &= \begin{bmatrix} x \\ \text{dz}(u) \end{bmatrix}^\top \left(\begin{bmatrix} A_{\text{cl}}^d(G^x) \\ B_{\text{cl}}^d \end{bmatrix}^\top P \begin{bmatrix} A_{\text{cl}}^d(G^x) & B_{\text{cl}}^d \end{bmatrix} - \begin{bmatrix} P & 0 \\ 0 & 0 \end{bmatrix} \right) \begin{bmatrix} x \\ \text{dz}(u) \end{bmatrix}. \end{aligned} \quad (22)$$

Exploiting the sector condition (16) for any x satisfying $\text{dz}(Hx) = 0$, we can upper bound

$$\Delta V(x) \leq \Delta V(x) + 2 \text{dz}(u)^\top W (Kx - \text{dz}(u) + Hx) = \xi^\top \Xi \xi, \quad (23)$$

where we denoted $\xi = \begin{bmatrix} x \\ \text{dz}(u) \end{bmatrix}$ and

$$\Xi = \text{He} \begin{bmatrix} -\frac{P}{2} & 0 & 0 \\ WK + WH & -W & 0 \\ X_{1,T}^d G^x & -B_{\text{cl}}^d & -\frac{P^{-1}}{2} \end{bmatrix}. \quad (24)$$

Based on the solution Q, F, M, N of (18), consider now the following selection of the variables appearing in (24),

$$P = Q^{-1} > 0, \quad G^x = F Q^{-1}, \quad (25a)$$

$$W = M^{-1} > 0 \text{ diagonal}, \quad H = N Q^{-1}, \quad (25b)$$

where positive definiteness of P follows from $Q = Q^\top > 0$ induced by the (1,1) entry of (18b), and positive definiteness of W is induced by the (2,2) entry of (18b). Then, pre- and post-multiplying (18b) by $\text{diag}\{P, W, I\}$, and accounting for the

selection of K in (19), we obtain $\Xi < 0$, which may be used in (23) to show that

$$dz(Hx) = 0 \implies \Delta V(x) \leq \lambda_M(\Xi)|x|^2 < 0, \quad (26)$$

with $\lambda_M(\Xi) < 0$ denoting the largest eigenvalue of (the negative definite matrix) Ξ .

Consider now pre- and post-multiplying (18a) by $\text{diag}\{P, 1\}$, which, exploiting (25), corresponds to

$$\begin{bmatrix} P & H_j^\top \\ H_j & \bar{u}_j^2 \end{bmatrix} \geq 0, \quad j = 1, \dots, n_u. \quad (27)$$

After a Schur complement, $\frac{H_j^\top H_j}{\bar{u}_j^2} \leq P$ for all such values of j , this clearly implies $x \in \mathcal{E}(Q, 1) \implies dz(Hx) = 0$, with $\mathcal{E}(Q, 1)$ defined in (20), which can be combined with (26) to show that $x \in \mathcal{E}(Q, 1) \setminus \{0\} \implies \Delta V(x) < 0$, completing the proof. ■

It is worth remarking that the design conditions (18a)-(18c) only depend on data and known features of the system under control. Indeed, the LMI in (18a) solely relies on the *known* saturation bound characterizing (3a). Instead, the LMI in (18b) and the equality condition in (18c) only depend on data and the DD description (10) of the closed loop dynamics.

Remark 2 (Feasibility & optimization): An interesting feature of the design conditions (18) is that they inherit the desirable feasibility properties of the model-based case analysed in [14]. In particular, a solution always exists under a mild (necessary) stabilizability condition for pair (A, B) . On the other hand, while feasibility is not an issue for the LMIs (18), the ensuing estimate (20) of the basin of attraction may result to be small. Due to this fact, following parallel derivations to the model-based scenario, we may include an additional LMI

$$\alpha I \leq Q, \quad (28)$$

ensuring the set inclusion $\{x : |x|^2 \leq \alpha\} \subset \mathcal{E}(Q, 1)$ (recall that $P = Q^{-1}$), so that maximizing α enlarges the size of $\mathcal{E}(Q, 1)$. The conditioning of $\mathcal{E}(Q, 1)$ may also be enforced to a maximum preassigned value $\kappa > 1$ by replacing (28) with $\alpha I \leq Q \leq \alpha \kappa I$. One may also maximize the volume of $\mathcal{E}(Q, 1)$ via “log det” optimization.

IV. HANDLING SATURATION WITH NOISY DATA

As discussed in Section III, the feasibility conditions in (18a)-(18c) are equivalent to their model-based counterparts in a deterministic setting only. Nonetheless, such a scenario is rather unrealistic in practice, since measurements are always corrupted by noise. Therefore, we now shift our attention to a (more realistic) scenario, where the available data are noisy according to (4). To this end, let us introduce the single row Hankel matrices $E_{0,T-1}$ and $E_{1,T}$, comprising the noise corrupting the state measurements.¹

Combining (3a) and (4), it can be seen that the considered data-generating system has an *output error* (OE) structure. As such, when noise comes into the picture, the model in (8) is biased as formalized in the following result.

¹Note that vectors $E_{0,T-1}$ and $E_{1,T}$ are not available for measurement.

Theorem 2: [On the consistency of (8)] With measurements (4) corrupted by zero-mean, white noise e , the open-loop model in (8) is asymptotically biased.

Proof: Based on (9), the data-based estimates of the matrices A and B in (3a) are given by:

$$\begin{bmatrix} \hat{B} & \hat{A} \end{bmatrix} = X_{1,T}^d \begin{bmatrix} V_{0,T-1}^d \\ X_{0,T-1}^d \end{bmatrix}^\dagger. \quad (29)$$

Nonetheless, according to (3a) and (4), the data $X_{1,T}^d$ can be replaced with the following expression:

$$X_{1,T}^d = \begin{bmatrix} B & A \end{bmatrix} \begin{bmatrix} V_{0,T-1}^d \\ X_{0,T-1}^d - E_{0,T-1} \end{bmatrix} + E_{1,T}, \quad (30)$$

where we have exploited (4) to replace the true (noise free) states $X_{0,T-1}$ driving $X_{1,T}^d$ with their noisy counterparts as

$$X_{0,T-1} = X_{0,T-1}^d - E_{0,T-1}. \quad (31)$$

As a consequence, (29) can be equivalently recast as

$$\begin{bmatrix} \hat{B} & \hat{A} \end{bmatrix} = \begin{bmatrix} B & A \end{bmatrix} + \underbrace{(E_{1,T} - AE_{0,T-1}) \begin{bmatrix} V_{0,T-1}^d \\ X_{0,T-1}^d \end{bmatrix}^\dagger}_{:= \varepsilon_T^d}, \quad (32)$$

where ε_T^d is the noise-induced bias. Let $\Delta E_{0,T} = E_{1,T} - AE_{0,T-1}$. By using standard system identification arguments [12], formulation (32) allows us to get

$$\lim_{T \rightarrow \infty} \frac{1}{T} \varepsilon_T^d = \lim_{T \rightarrow \infty} \frac{\Delta E_{0,T}}{T} \begin{bmatrix} 0 \\ E_{0,T-1} \end{bmatrix}^\top \left(\begin{bmatrix} V_{0,T-1}^d \\ X_{0,T-1}^d \end{bmatrix} \begin{bmatrix} V_{0,T-1}^d \\ X_{0,T-1}^d \end{bmatrix}^\top \right)^{-1} \neq 0,$$

almost surely, due to its dependence on the product between $E_{0,T-1}$ and its transpose. ■

By using (10) in the noisy case, we thus disregard the asymptotic result in Theorem 2, injecting the bias appearing in (32) into the closed-loop representation used for DD control design. This choice, in turn, might severely influence the design, potentially jeopardizing closed-loop stability. To overcome this problem, we initially exploit an instrumental variable scheme [12] to recast (8).

Let us assume that we can perform an additional experiment, by using the *same* input exploited in the construction of the sequence \mathcal{V}_T in \mathcal{D}_T . This experiment results in an additional state sequence $\tilde{\mathcal{X}}_T = \{\tilde{x}^d(t)\}_{t=0}^T$ made of the *same noiseless states* constituting \mathcal{X}_T in \mathcal{D}_T , but corrupted by a different realization of the noise. We then use this new state sequence to construct the *instrument*

$$Z_{0,T-1}^d = \begin{bmatrix} V_{0,T-1}^d \\ \tilde{X}_{0,T-1}^d \end{bmatrix}, \quad (33)$$

which is uncorrelated with the noises $E_{1,T}$ and $E_{0,T-1}$ corrupting the states in the initial dataset, while satisfying the conditions (6)-(7) by construction. The instrument allows us to recast the DD open-loop description of the system as:

$$x^+ = X_{1,T}^d (Z_{0,T-1}^d)^\top \left(\begin{bmatrix} V_{0,T-1}^d \\ X_{0,T-1}^d \end{bmatrix} (Z_{0,T-1}^d)^\top \right)^{-1} \begin{bmatrix} \text{sat}(u) \\ x \end{bmatrix}, \quad (34)$$

as formalized in the following Lemma.

Lemma 4 (DD open-loop with noise): Given the *unknown* system in (3a), a sufficiently long (in the sense of (6)) set of *noisy data* $\mathcal{D}_T = \{\mathcal{V}_T, \mathcal{X}_T\}$, with \mathcal{V}_T being persistently exciting of order $n_x + 1$, and the instrument $Z_{0,T-1}^d$ in (33), then (34) is asymptotically equivalent to (3a), *i.e.*,

$$\lim_{T \rightarrow \infty} X_{1,T}^d (Z_{0,T-1}^d)^\top \left(\begin{bmatrix} V_{0,T-1}^d \\ X_{0,T-1}^d \end{bmatrix} (Z_{0,T-1}^d)^\top \right)^{-1} = [B \ A], \quad (35)$$

almost surely.

Proof: The open-loop description in (34) stems from the solution of the following instrumental variable problem

$$\text{minimize} \left\| \begin{bmatrix} X_{1,T}^d - [B \ A] \begin{bmatrix} V_{0,T-1}^d \\ X_{0,T-1}^d \end{bmatrix} \\ [B \ A] \end{bmatrix} (Z_{0,T-1}^d)^\top \right\|_F, \quad (36)$$

from which it results that

$$[\hat{B} \ \hat{A}] = X_{1,T}^d (Z_{0,T-1}^d)^\top \left(\begin{bmatrix} V_{0,T-1}^d \\ X_{0,T-1}^d \end{bmatrix} (Z_{0,T-1}^d)^\top \right)^{-1}. \quad (37)$$

Decomposing $X_{0,T-1}^d$ as in (30)-(31), we obtain that

$$[\hat{B} \ \hat{A}] = [B \ A] + \underbrace{\Delta E_{0,T-1} (Z_{0,T-1}^d)^\top \left(\begin{bmatrix} V_{0,T-1}^d \\ X_{0,T-1}^d \end{bmatrix} (Z_{0,T-1}^d)^\top \right)^{-1}}_{:= \tilde{\varepsilon}_T^d},$$

where $\Delta E_{0,T} = E_{1,T} - A E_{0,T-1}$. Thanks to the choice of the instrument, it then holds that

$$\lim_{T \rightarrow \infty} \frac{1}{T} \tilde{\varepsilon}_T^d = \lim_{T \rightarrow \infty} \frac{\Delta E_{0,T}}{T} \begin{bmatrix} 0 \\ \tilde{E}_{0,T-1} \end{bmatrix}^\top \left(\begin{bmatrix} V_{0,T-1}^d \\ X_{0,T-1}^d \end{bmatrix} (Z_{0,T-1}^d)^\top \right)^{-1} = 0,$$

where $\tilde{E}_{0,T-1}$ is the realization of the noise characterizing the instrument, which is uncorrelated with $E_{0,T-1}$ and $E_{1,T}$ by construction, thus concluding the proof. \blacksquare

According to Lemma 4, we can then construct an alternative closed-loop representation with noisy data, given by

$$x^+ = \tilde{A}_{cl}^d(\tilde{G}^x) x + \tilde{B}_{cl}^d dz(Kx), \quad (38a)$$

with

$$\tilde{A}_{cl}^d(\tilde{G}^x) = X_{1,T}^d (Z_{0,T-1}^d)^\top \tilde{G}^x, \quad (38b)$$

$$\tilde{B}_{cl}^d = X_{1,T}^d (Z_{0,T-1}^d)^\top \left(\begin{bmatrix} V_{0,T-1}^d \\ X_{0,T-1}^d \end{bmatrix} (Z_{0,T-1}^d)^\top \right)^{-1} \begin{bmatrix} I \\ 0 \end{bmatrix}, \quad (38c)$$

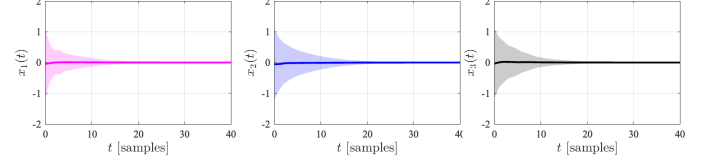
and $\tilde{G}^x \in \mathbb{R}^{n_x + n_u \times n_x}$ satisfying

$$\begin{bmatrix} K \\ I \end{bmatrix} = \begin{bmatrix} V_{0,T-1}^d \\ X_{0,T-1}^d \end{bmatrix} (Z_{0,T-1}^d)^\top \tilde{G}^x. \quad (38d)$$

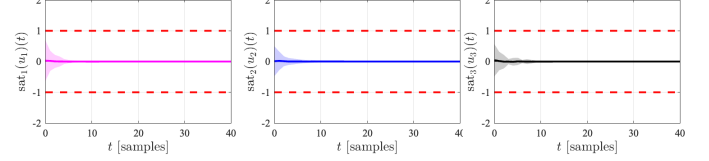
This result is formalized next.

Theorem 3 (DD closed-loop with noise): Consider the *unknown* system (3a), a sufficiently long (in the sense of (6)) set of *noisy data* $\mathcal{D}_T = \{\mathcal{V}_T, \mathcal{X}_T\}$, with \mathcal{V}_T being persistently exciting of order $n_x + 1$ and the instrument $Z_{0,T-1}^d$ in (33). The closed loop (3), (5) is asymptotically equivalent to (38a).

Proof: The proof follows similar steps to those of the proof of Lemma 3, in particular, thanks to the rank condition

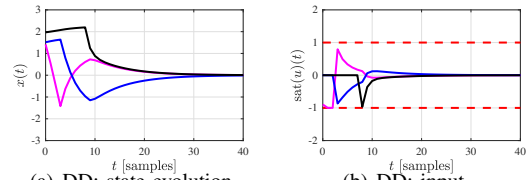


(a) DD: state evolution



(b) DD: input

Fig. 2. Mean and standard deviation (shaded area) of states and inputs over the 97 realizations of the initial condition leading to non-diverging trajectories. The red dashed lines indicate the saturation limits \bar{u} .



(a) DD: state evolution

(b) DD: input

Fig. 3. States/inputs trajectories for one initial condition: first (magenta), second (blue), third (black) components; saturation limits (dashed red).

(7), we can define \tilde{G}^x as in (38d). Thus, the closed-loop transition matrix $\tilde{A}_{cl}^d(\tilde{G}^x)$ becomes:

$$\begin{aligned} \tilde{A}_{cl}^d(\tilde{G}^x) &= X_{1,T}^d (Z_{0,T-1}^d)^\top \left(\begin{bmatrix} V_{0,T-1}^d \\ X_{0,T-1}^d \end{bmatrix} (Z_{0,T-1}^d)^\top \right)^{-1} \begin{bmatrix} K \\ I \end{bmatrix} \\ &= X_{1,T}^d (Z_{0,T-1}^d)^\top \tilde{G}^x, \end{aligned}$$

and the remaining terms in (38) easily follow. \blacksquare

Note that this closed-loop description still exploits a (now asymptotically unbiased) estimate of B , while the matrix $\tilde{A}_{cl}^d(\tilde{G}^x)$ enjoys the same form as in (15b), except for the dependence on the instrument. Due to this change, the design condition (18b) should be replaced by

$$\text{He} \left(\begin{bmatrix} -\frac{Q}{2} & 0 & 0 \\ V_{0,T-1}^d (Z_{0,T-1}^d)^\top \tilde{F} + N & -M & 0 \\ X_{1,T}^d (Z_{0,T-1}^d)^\top \tilde{F} & -\tilde{B}_{cl}^d M & -\frac{Q}{2} \end{bmatrix} \right) < 0, \quad (39)$$

where $\tilde{F} = \tilde{G}^x Q$, and (18c) generalizes to:

$$X_{0,T-1}^d (Z_{0,T-1}^d)^\top \tilde{F} = Q. \quad (40)$$

Remark 3 (On the length of the dataset): The consistency of the closed-loop representation (38) is only guaranteed asymptotically (*i.e.*, as $T \rightarrow \infty$). At the same time, differently from the deterministic model in (38a), T does not dictate the dimension of the variable \tilde{G}^x (and, thus, \tilde{F}) any longer. As a consequence, the dataset T can in principle be arbitrary long.

V. NUMERICAL EXPERIMENTS

Let us consider the open-loop unstable, LTI system \mathcal{S} with fully measurable state considered in [4], with

$$A = \begin{bmatrix} 1.01 & 0.01 & 0 \\ 0.01 & 1.01 & 0.01 \\ 0 & 0.01 & 1.01 \end{bmatrix}, \quad B = I.$$

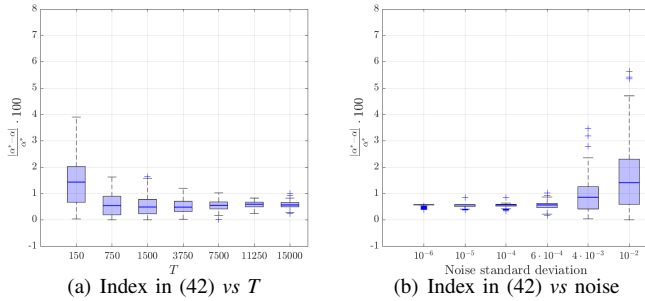


Fig. 4. Performance index vs increasing noise and dataset length.

TABLE I

NUMBER OF INSTANCES IN WHICH (43) IS SATISFIED VS LENGTH OF THE DATASET T OVER 100 REALIZATIONS OF \mathcal{D}_T

T [samples]	150	750	1500	7500	11250	15000
eq. (43) satisfied	42	48	58	82	84	97

This system is in cascade with a saturation, with \bar{u} in (3b) equal to 1. Since the system is open-loop unstable, the dataset \mathcal{D}_T is collected in closed-loop. Specifically, the system is stabilized by a feedback law (5) with $K = I$ and a closed-loop experiment (of length $T = 6000$ steps) is carried out by considering a random reference to be tracked, that is uniformly distributed within the interval $[-1, 1]$. It is worth pointing out that the length and the features of the chosen input sequence guarantee the necessary level of persistence of excitation (according to Definition 1). In addition, the available state measurements are corrupted by zero-mean white noise with standard deviation $0.02I$. In designing the feedback law in (5), we solve²

$$\underset{\alpha}{\text{minimize}} \quad -\alpha \quad (41a)$$

$$\text{s.t. (18a), (28), (39) – (40).} \quad (41b)$$

By considering 100 initial conditions, extracted uniformly at random within $[-2, 2]$, we initially assess the performance of the proposed DD strategy by looking at the closed-loop state and input trajectories³. As shown in Fig. 2, the states settle to zero after about 40 steps, independently of the considered realization of the initial condition. Meanwhile, the input fed to the plant is saturated only few times at the beginning of the simulation horizon, with this sporadic behavior being not evident in Fig. 2. Focusing on a specific initial condition (see Fig. 3), it is nonetheless clear that the DD control law allows the input to recover from saturation, ultimately enabling the states to converge to zero⁴.

We now evaluate the performance of the proposed DD design approach against the dimension \mathcal{D}_T , considering 100 realizations of the dataset for each of the tested values of T and setting the standard deviation of the noise to $10^{-3}I$. To this end, we consider the following quality index

$$\frac{|\alpha^* - \alpha|}{\alpha^*} \cdot 100 \quad (42)$$

²The design problem was solved with Yalmip+SeDuMi [11], [13].

³We do not inject noise into the closed-loop, when performing these tests.

⁴Only 3 out of 100 initial conditions lead to diverging closed-loop states with the DD controller, while initial conditions resulting in diverging states increase to 6 when using system identification (36) and model-based design.

TABLE II

NUMBER OF INSTANCES IN WHICH (43) IS SATISFIED VS NOISE STANDARD DEVIATION OVER 100 REALIZATIONS OF \mathcal{D}_T .

Noise std	10^{-6}	10^{-5}	10^{-4}	$6 \cdot 10^{-4}$	$4 \cdot 10^{-3}$	10^{-2}
eq. (43) satisfied	100	100	100	98	55	41

measuring the capability of the DD approach to result in a cost (41a) that is comparable to that of the *oracle* (i.e., model-based) solution, in turn dictated by α^* . As shown in Fig. 4(a), by increasing the dimension of the dataset used for DD design, the cost of the DD solution progressively matches that of the model-based one, while closed-loop state trajectories (starting from $x_i(0) = 1.5$, $i = 1, 2, 3$) always converge to the origin. Meanwhile, we check the condition

$$Q^* - Q \succeq 0, \quad (43)$$

where Q^* and Q respectively dictate the *oracle* (model-based) and the DD characterization of (20), which implies that the data-driven estimate $\mathcal{E}(Q, 1)$ contains the *oracle*-based estimate $\mathcal{E}(Q^*, 1)$. Clearly, the more T increases, the more times this condition is satisfied (see Table I). These behaviors are in line with the asymptotic properties associated with the employed instrumental variable scheme of Lemma 4. Finally, we assess the performance of the proposed DD approach for increasing levels of noise, when $T = 6000$. From the results reported in Fig. 4(b), it is clear that the value of the quality index in (42) increases (worsens) with the level of noise, along with the number of instances in which (43) is not satisfied. Note that all state trajectories always converge to zero.

VI. CONCLUSIONS

In this work we proposed a data-based strategy for the design of a regionally stabilizing controller for input-saturated plants by relying on generalized sector conditions. To handle noise, we proposed an instrumental variable approach that leads to an asymptotically unbiased description of the closed-loop system. Future research will be devoted to extend the proposed approach to a purely input/output setting and to explore its finite sample properties.

REFERENCES

- [1] J. Berberich, J. Köhler, M.A. Müller, and F. Allgöwer. Data-driven model predictive control with stability and robustness guarantees. *IEEE Transactions on Automatic Control*, 66(4):1702–1717, 2021.
- [2] V. Breschi, A. Chiuso, and S. Formentin. Data-driven predictive control in a stochastic setting: a unified framework. *arXiv:2203.10846*, 2022.
- [3] V. Breschi and S. Formentin. Direct Data-Driven Control with Embedded Anti-Windup Compensation. In *Proceedings of the 2nd Conference on Learning for Dynamics and Control*, volume 120 of *Proceedings of Machine Learning Research*, pages 46–54. PMLR, 2020.
- [4] V. Breschi, D. Masti, S. Formentin, and A. Bemporad. NAW-NET: neural anti-windup control for saturated nonlinear systems. In *59th IEEE Conference on Decision and Control (CDC)*, pages 3335–3340, 2020.
- [5] M.C. Campi, A. Lecchini, and S.M. Savaresi. Virtual reference feedback tuning: a direct method for the design of feedback controllers. *Automatica*, 38(8):1337–1346, 2002.
- [6] J. Coulson, J. Lygeros, and F. Dörfler. Data-enabled predictive control: In the shallows of the DeepPC. In *2019 18th European Control Conference (ECC)*, pages 307–312, 2019.
- [7] C. De Persis and P. Tesi. Formulas for Data-Driven Control: Stabilization, Optimality, and Robustness. *IEEE Transactions on Automatic Control*, 65(3):909–924, 2020.

- [8] C. De Persis and P. Tesi. Low-complexity learning of Linear Quadratic Regulators from noisy data. *Automatica*, 128:109548, 2021.
- [9] F. Dörfler, P. Tesi, and C. De Persis. On the Certainty-Equivalence Approach to Direct Data-Driven LQR Design, 2021. 10.48550/ARXIV.2109.06643.
- [10] H. Hjalmarsson. Iterative feedback tuning—an overview. *Int. Journal of Adaptive Control and Signal Processing*, 16(5):373–395, 2002.
- [11] J. Löfberg. YALMIP : A Toolbox for Modeling and Optimization in MATLAB. In *In Proceedings of the CACSD Conference*, 2004.
- [12] T. Söderström and P. Stoica. Instrumental variable methods for system identification. *Circuits, Systems and Signal Processing*, 21(1):1–9, 2002.
- [13] J.F. Sturm. Using SeDuMi 1.02, a MATLAB toolbox for optimization over symmetric cones. *Opt. meth. and software*, 11(1-4):625–653, 1999.
- [14] S. Tarbouriech, G. Garcia, J.M. Gomes da Silva Jr., and I. Queinnec. *Stability and stabilization of linear systems with saturating actuators*. Springer-Verlag London Ltd., 2011.
- [15] J. van Wingerden, S. Mulders, R. Dinkla, T. Oomen, and M. Verhaegen. Data-enabled predictive control with instrumental variables: the direct equivalence with subspace predictive control, 2022. 10.48550/arxiv.2209.05210.
- [16] J.C. Willems, P. Rapisarda, I. Markovsky, and B. De Moor. A note on persistency of excitation. *Syst. & Control Letters*, 54(4):325–329, 2005.
- [17] L. Zaccarian and A.R. Teel. *Modern anti-windup synthesis: control augmentation for actuator saturation*. Princeton University Press, Princeton (NJ), 2011.